applied optics

Improved method to fully compensate the spatial phase nonuniformity of LCoS devices with a Fizeau interferometer

Qiang Lu,[1,2,*] Lei Sheng,[1] Fei Zeng,[1] Shijie Gao,[1] and Yanfeng Qiao[1]

[1]Changchun Institute of Optics, Fine Mechanics and Physics, Chinese Academy of Sciences, Dongnanhu Road 3888, Changchun 130033, China
[2]University of Chinese Academy of Sciences, Beijing 100049, China
*Corresponding author: luqiang52177@163.com

Received 30 June 2016; revised 16 August 2016; accepted 30 August 2016; posted 30 August 2016 (Doc. ID 269517); published 22 September 2016

Liquid crystal on silicon (LCoS) devices usually show spatial phase nonuniformity (SPNU) in applications of phase modulation, which comprises the phase retardance nonuniformity (PRNU) as a function of the applied voltage and inherent wavefront distortion (WFD) introduced by the device itself. We propose a multipoint calibration method utilizing a Fizeau interferometer to compensate SPNU of the device. Calibration of PRNU is realized by defining a grid of 3×6 cells onto the aperture and then calculating phase retardance of each cell versus a gradient gray pattern. With designing an adjusted gray pattern calculated by the calibrated multipoint phase retardance function, compensation of inherent WFD is achieved. The peak-to-valley (PV) value of the residual WFD compensated by the multipoint calibration method is significantly reduced from 2.5λ to 0.140λ, while the PV value of the residual WFD after global calibration is reduced to 0.364λ. Experimental results of the generated finite-energy 2D Airy beams in Fourier space demonstrate the effectiveness of this multipoint calibration method. © 2016 Optical Society of America

OCIS codes: (230.3720) Liquid-crystal devices; (220.1000) Aberration compensation; (050.1970) Diffractive optics.

http://dx.doi.org/10.1364/AO.55.007796

1. INTRODUCTION

Spatial light modulator (SLM) technology based on liquid crystal (LC) on silicon devices has been an active area of research in recent years [1]. It is now well known that LCoS devices allow both amplitude modulation and phase modulation [2]. Unlike amplitude modulation, LCoS devices in phase-only modulation mode have a wide range of applications, including adaptive optics [3,4], diffractive optical elements (DOEs) [5], micromanipulations [6], optical tweezers [7], and holographic displays [8].

Phase-only modulating LCoS devices usually show characteristics of spatial phase nonuniformity in the applications. The SPNU of LCoS devices consist of phase retardance nonuniformity (PRNU) as a function of the applied voltage and inherent wavefront distortion (WFD). The reason for PRNU is the thickness variation of the LC layer [9], which is mainly caused by the curvature of silicon backplane. Due to manufacturing process on the wafer scale, single LCoS device cells show a residual bending of their silicon backplane as a result of the dicing process [10]. Meanwhile, the inherent WFD of the device is caused by the curvature of the silicon backplane and the thickness variations of the glass substrate and LC layer, which is introduced to the incident wavefront. In order to acquire a desired optical performance, compensation of SPNU is an essential procedure when utilizing phase-only LCoS devices for phase profile modulation.

Different methods were reported to calibrate PRNU of the LCoS device, such as the crossed-polarizers (C-P) method [11,12] and the diffraction-based calibration method [13]. However, these two methods fail to measure and compensate the inherent WFD by themselves. Another method is needed to fully compensate SPNU of the LCoS device. To solve this problem, the Michelson interferometer method was proposed to measure the WFD of the LCoS device [12,14]. However, the measured results contain additional wavefront distortions caused by other optical components, like the beam splitter, in the test system, which degrades the accuracy of the results. Recently, a thickness-calibration-based compensation method was presented, which corrects both the anisotropic and isotropic nonuniformities of the LC layer [15]. However, this method merely focuses on the compensation of the phase nonuniformity of LC layer. The inherent WFD caused by the thickness variation of glass substrate and the curvature of silicon backplane is not taken into account.

The multipoint phase calibration method has been proven as an efficient and time-saving method. Unlike the

pixel-to-pixel compensation method, it defines a grid of cells onto the LCoS aperture to develop a multipoint calibration, under the condition that the phase response of each cell is nonabrupt [16]. However, calibrating each cell of the defined grid is troublesome work because each cell still needs to be measured once while varying the addressed gray level from 0 to 255 every time. Therefore, a simple and time-saving method to fully calibrate the SPNU of the LCoS device is urgently required.

In this paper, we present a multipoint calibration method based on a Fizeau interferometer to fully compensate SPNU of the LCoS device. The calibration method is achieved by directly measuring the phase retardance with the help of an absolute phase reference in the optical system, rather than depending on the conventional combination of the C-P method and the Michelson interferometer method. In phase-only modulation mode, the phase modulation mechanism can be interpreted as superimposing the phase retardance versus the applied voltage and the inherent WFD to the incident wavefront. Thus, an absolute phase reference in the optical system is introduced to measure the inherent WFD by a four-step phase-shift interferometry algorithm. To calibrate PRNU of the device, we define a grid of cells onto the LCoS aperture and design a gradient gray pattern with the gray level varying from 0 to 255 along the horizontal axis in each cell area. By loading the special gray pattern to the device instead of changing the gray level from 0 to 255 during the calibration procedure, it only needs to measure a few times. Moreover, the relative phase retardances corresponding to the addressed gray level from 0 to 255 of each cell can be directly obtained using the Fizeau interferometer. Also, compensation of the inherent WFD and the measured results of the residual WFD after phase compensation will be demonstrated, which is followed by the generation of finite-energy 2D Airy beams in Fourier space.

2. COMPENSATION PRINCIPLE AND PROCEDURE

The LCoS device used in this paper is a reflective device, which is manufactured by Holoeye, Inc. The device panel has 1920 × 1080 pixels in a 15.36 mm × 8.64 mm array, with a pixel pitch of 8 μm × 8 μm, 60% 0th diffraction efficiency, and 87% fill factor.

In phase-only modulation mode, a single polarizer (S-P) is used in the setup to ensure the polarized direction of the incident light parallel with the long axis directions of LC molecules. When the linearly polarized light passes through the LCoS device, modulation of the incident wavefront is accomplished by changing the reorientation of LC molecules using voltage. Normally, the applied voltage V is translated into 8 bit gray level h as

$$h = h_{\min} + \frac{h_{\max} - h_{\min}}{V_{\max} - V_{\min}} \times V, \tag{1}$$

where $h_{\max} = 255$, $h_{\min} = 0$, $V_{\max} = 4.19$ V, and $V_{\min} = 0.03$ V of this LCoS device.

Figures 1(a) and 1(b) illustrate the total phase retardance of the LCoS device for $V = 0$ and $V > 0$. When the applied voltage $V = 0$, as shown in Fig. 1(a), the total phase retardance across the aperture is the inherent WFD, Φ_{WFD}, which is

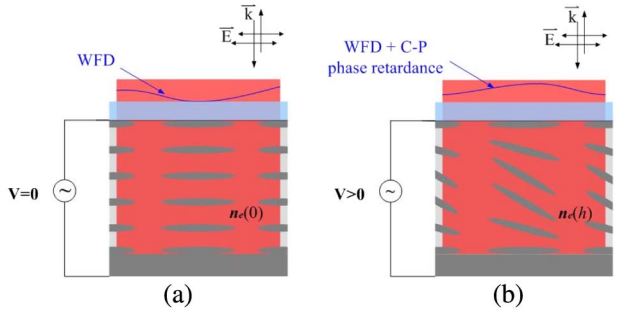

Fig. 1. Illustration of the total phase retardance of the LCoS device when the direction of the incident light is parallel to the plane as the long axis of the LC molecules. (a) $V = 0$, the total phase retardance is the inherent WFD. (b) $V > 0$, the total phase retardance is the sum of inherent WFD and C-P phase retardance.

caused by the curvature of the silicon backplane and the thickness variations of the glass substrate and LC layer. When the applied voltage $V > 0$, phase retardance is obtained due to the change of the extraordinary refractive index $n_e(h)$. The phase retardance as a function of the addressed gray level is called as the C-P phase retardance [12], $\Delta\Phi_{\mathrm{LC}}(h)$, expressed by

$$\begin{aligned}\Delta\Phi_{\mathrm{LC}}(h) &= 2\pi\frac{2d_{\mathrm{LC}}[n_e(h) - n(0)]}{\lambda} \\ &= 2\pi\frac{2d_{\mathrm{LC}}\Delta n_e(h)}{\lambda},\end{aligned} \tag{2}$$

where d_{LC} is the thickness of the LC layer, λ is the wavelength, and $\Delta n_e(h)$ is the birefringent value. In this case, the total phase retardance consists of the inherent WFD and the C-P phase retardance, as shown in Fig. 1(b), which can be expressed as

$$\Phi = \Phi_{\mathrm{WFD}} + \Delta\Phi_{\mathrm{LC}}(h). \tag{3}$$

According to Eq. (3), if we measure the inherent WFD of the LCoS device and calibrate the phase retardance function separately, the corresponding total phase retardance of a pixel can be calculated. Thus, the SPNU of the LCoS device is fully corrected. To solve this problem, an absolute phase reference in a Fizeau interferometer is introduced. The Fizeau interferometer measures the relative phase to the phase reference only, if the full aperture is loaded with the same gray level, the measured phase response is not the C-P phase retardance but the phase response nonuniformity across the aperture versus the same addressed gray level and inherent WFD. To calibrate the phase retardance function, a special gradient gray pattern with the gray level varying from 0 to 255 along the horizontal axis is designed. In this way, the C-P phase retardance versus the gray level from 0 to 255 along the horizontal axis is measured. Meanwhile, a grid of cells is defined onto the aperture of the device to develop a multipoint calibration using this method.

An illustration of the procedure to compensate SPNU of the LCoS device based on a Fizeau interferometer is shown in Fig. 2. To begin with, the inherent WFD is measured by the Fizeau interferometer directly when the applied voltage $V = 0$. Then, with loading the special gradient gray pattern we designed onto the device, the corresponding multipoint phase retardance function is calibrated by using the measured

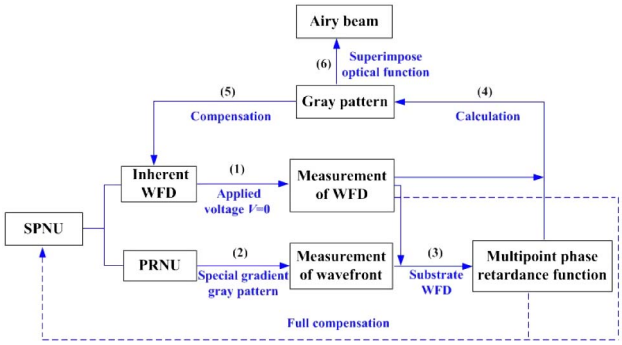

Fig. 2. Procedure to compensate SPNU of the LCoS device based on a Fizeau interferometer.

wavefront to subtract the inherent WFD. After that, a compensation gray pattern can be computed using the calibrated multipoint phase retardance function to modulate the phase values across the aperture to the same phase value, and it is equal to the maximum phase value of the inherent WFD. With these three steps, the SPNU of the LCoS device is compensated. Finally, an optical function can be superimposed to the compensation phase function like a 2D Airy beam if necessary.

3. OPTICAL SYSTEM

A Fizeau interferometer introducing an absolute phase reference is one of the most important parts to compensate SPNU of the LCoS device in this paper. Figure 3 basically shows a Fizeau interferometer with the LCoS device in front of the referenced transmission flat. The phase responses are measured by a four-step phase-shift interferometry algorithm, in which the transmission flat is shifted in four $\lambda/4$ steps to produce four interferograms. The advantage of the Fizeau interferometer is the transmitted beam, and the reflected beam shares a common optical path, as shown in Fig. 3, so the phase difference between them is only double the WFD caused by the

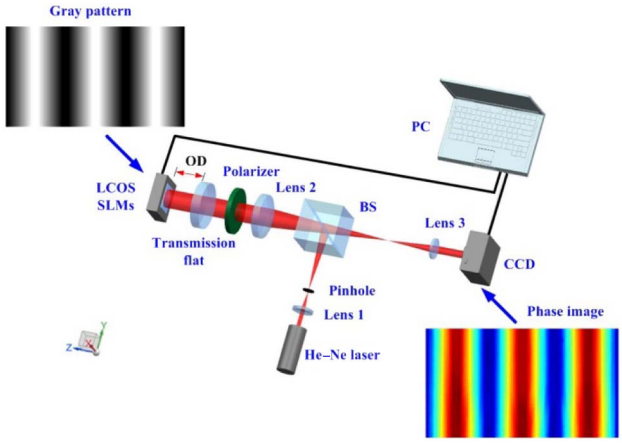

Fig. 3. Schematic of the optical system to measure the SPNU characteristics of the LCoS device, where the He–Ne laser is a collimated 632.8 nm laser, lens 1 to lens 3 are the lenses, BS is the beam splitter, and Transmission flat is a phase reference (flatter than $\lambda/20$ at the wavelength of 632.8 nm).

LCoS device. In this way, it is capable of removing wavefront distortions introduced by other optical components in the optical system. This is different from the conventional Michelson interferometer.

The operation of the optical system in Fig. 3 can be described as follows. A collimated He–Ne (632.8 nm) laser beam is focused on a pinhole by lens 1. Then the beam passes through a beam splitter (BS), where half of the beam is reflected to a collimated lens 2. Following lens 2 is a polarizer which ensures the polarized direction of the incident beam parallel with the long axis directions of the LC molecules. A referenced transmission flat is included in this system, which is optimized for 4:96 beam splitting at vertical incidence. After the transmission flat, part of the beam is directly reflected back to lens 3, a collimated lens, whose function is to collimate the focal beam caused by lens 2. The other part of the beam is further imaged onto the LCoS device. The wavefront of the transmitted beam is modulated by the LCoS device and then interferes with the former reflected beam. Finally, the interferogram is imaged on the CCD camera. In the experiments, interferograms of 1920 × 1080 LCoS pixels are all imaged on 380 × 214 pixels of the CCD. The size of a CCD pixel is 14 μm, and the used area of the CCD is 5.32 mm × 3.00 mm. As the sizes of SLM and CCD are different, we use lens 2 and lens 3 to constitute a 2.8 times beam expander system to adjust the scale.

4. CALIBRATION OF PRNU

A. Measurement of Inherent WFD

The basic step of the compensation procedure for SPNU of the LCoS device is the measurement of inherent WFD. When the applied voltage $V = 0$, the distorted wavefront introduced by the device interfering with the referenced wavefront is imaged on CCD, as shown in Fig. 4(a). It can be seen that the interferential fringes are bent. This is the evidence of inherent WFD of the LCoS device. The deformation is mainly spherical and no more than 3λ at the wavelength of 632.8 nm for this used phase-only panel.

Phase distribution of inherent WFD measured by the Fizeau interferometer is shown in Fig. 4(b). The peak-to-valley (PV) value of the inherent WFD is about 2.5λ at the wavelength of 632.8 nm. The measured wavefront includes full WFD introduced by the LCoS device, which is caused by the curvature of

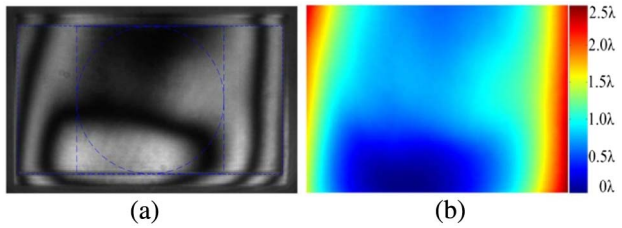

Fig. 4. (a) Interferogram comes from the referenced wavefront and the inherent WFD caused by the LCoS device, where the dashed rectangle stands for the measurement area of 1920 × 1080 LCoS pixels, and the square area and circular area are the usually used apertures. (b) Phase distribution of inherent WFD measured by the Fizeau interferometer.

the silicon backplane and the thickness variations of the LC layer and glass substrate.

B. Global Calibration of PRNU

In most applications, we usually assume that the phase retardance as a function of the addressed gray level is nonabrupt across the aperture. In this case, a global phase retardance function is achieved by loading the gray pattern shown in Fig. 5(a) to the device. It is a gradient gray pattern with the gray level varying from 0 to 255 along the horizontal axis. Figure 5(b) demonstrates the corresponding phase response, which is the difference between the measured wavefront and the inherent WFD in Fig. 4(b). The ellipses in Fig. 5(b) indicate the areas of different phase values along the vertical axis. It means the PRNU of the LCoS device.

In Fig. 6, the global phase retardance function is obtained by averaging the phase values along the vertical axis in Fig. 5(b) and fitting with the 8 bit gray level. It is noted that the phase modulation depth of this device is about 3.2λ at the wavelength of 632.8 nm.

C. Multipoint Calibration of PRNU

From the procedure of the global calibration method, we see that every point in Fig. 6 is the average of the phase retardances along the vertical axis in Fig. 5(b). Actually, the global calibration method only considers the PRNU along the vertical axis of the device. If addressing a scaled gray pattern of Fig. 5(a) onto a small area of the aperture, a phase retardance function for the small target area can be acquired. In this way, the device aperture is divided into some small areas to develop a multipoint calibration method. What counts is that the PRNU along the horizontal axis of the device is also taken into account by the multipoint calibration method.

It is noticed that the way to compute the measurement data in Fig. 5(b) is the average of the phase response values along the vertical axis of each cell. This is because the gray pattern that we designed varies from 0 to 255 (or from 255 to 0) along the horizontal axis, which we assume that the phase retardance along the vertical axis of each cell is nonabrupt. It indicates that the numbers of the rows along the vertical axis can be large enough without limitation and can even be 214 in theory. In fact, with the number of the rows increasing, there is a marginal improvement in the compensation results. The main reason for it is the influence of the environment in the experiment.

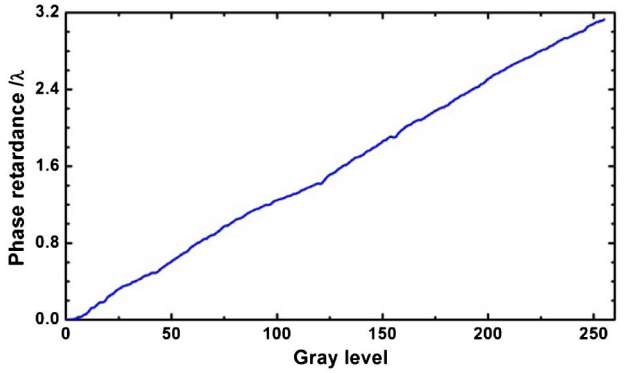

Fig. 6. Global phase retardance as a function of the gray level from 0 to 255 obtained by averaging the phase values along the vertical axis in Fig. 5(b) and fitting with the 8 bit gray level.

In order to collect enough data points along the horizontal axis to fit the phase retardance curve of each cell, the numbers of the columns along the horizontal axis cannot be large. The optimum number of columns should be chosen depending on the expander system, the resolution of the CCD, and the LCoS conditions. In the experiments, interferograms of 1920×1080 LCoS pixels are all imaged on 380×214 CCD pixels, and the number of the beam expander system is 2.8. Thus, we finally choose a grid of 3×6 cells defined onto the device aperture.

In this paper, the aperture of the LCoS device is divided into 18 small areas. To simplify the multipoint calibration method, a special gray pattern is designed, as shown in Fig. 7(a). The distribution of the gray level in each cell is equal along the vertical axis, and grades from 0 to 255 (or from 255 to 0) along the horizontal axis. Figure 7(b) illustrates the calculated wavefront result corresponding to the addressed gray pattern in Fig. 7(a). The arrows in Fig. 7(b) point out the obvious areas of PRNU.

By averaging the phase values along the vertical axis of each cell in Fig. 7(b) and fitting with the 8 bit gray level, a set of 18 phase retardance curves are obtained. Typical comparison with the phase retardance curves of the first row obtained by the multipoint calibration method with the curve obtained by the global calibration method are shown in Fig. 8.

It is obvious that all the phase retardance curves in Fig. 8 are almost linear. The difference of the phase retardances versus the same gray level is no more than 0.2λ (632.8 nm).

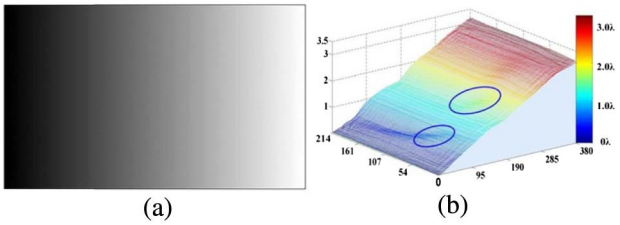

Fig. 5. (a) A gradient gray pattern with the gray level ranges from 0 to 255 along the horizontal axis, black is 0, white is 255. (b) 3D phase distribution of phase responses corresponds to the gray pattern in Fig. 5(a), which is the difference between the measured wavefront and the inherent WFD in Fig. 4(b). The ellipses denote the obvious areas of different phase values along the vertical axis in Fig. 5(b).

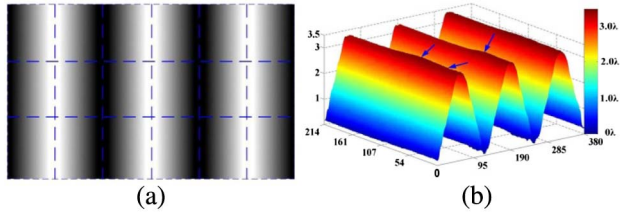

Fig. 7. (a) A special gray pattern designed for the multipoint calibration method, where black is 0, white is 255, and the dashed lines point out the defined grid of 3×6 cells on the aperture. (b) 3D phase distribution of the calculated wavefront result corresponding to the addressed gray pattern in Fig. 7(a). The arrows in Fig. 7(b) point out the obvious areas of PRNU.

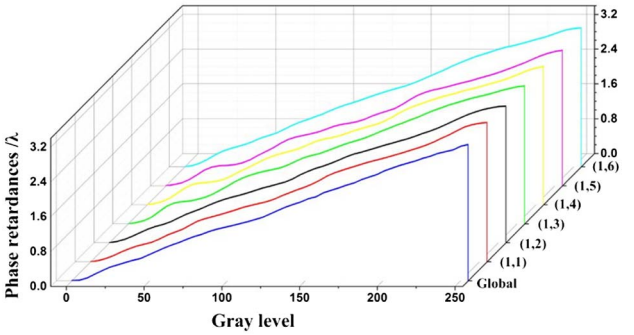

Fig. 8. Plots of the phase retardance versus the 8 bit gray level of the first row, which are obtained by the multipoint calibration method compared with the phase retardance curve obtained by the global calibration method. Global denotes the global phase retardance function as seen in Fig. 6. Coordinates (1,1) to (1,6) denote the corresponding measurement cells in the first row of Fig. 7(a).

5. COMPENSATION OF WFD

With the calibrated multipoint phase retardance function and the measured inherent WFD of the device, compensation of the distorted wavefront introduced to the incident light after passing through the LCoS device can be realized. To compensate it, a gray pattern to modulate the total phase retardance of every pixel to the same value, Φ_{max}, is computed. Φ_{max} is the maximum phase value of the WFD in Fig. 4(b). Thus, Eq. (3) can be described as

$$\Phi_{max} - \Phi_{WFD} = \Delta\Phi_{LC}(h), \quad (4)$$

where the C-P phase retardance of every pixel is the difference between the maximum phase value and the corresponding phase value of the inherent WFD in Fig. 4(b). The gray level of a pixel can be obtained by the calibrated phase retardance function. Figures 9(a) and 9(b) show the 2D gray patterns calculated using the global phase retardance function and the multipoint phase retardance function to compensate inherent WFD caused by the LCoS device. In Figs. 9(c) and 9(d), we show the interferograms after phase compensation with loading the gray patterns in Figs. 9(a) and 9(b).

After compensation, it can be seen that the interferograms both in Figs. 9(c) and 9(d) are almost the same intensity value across the aperture, which denotes that the inherent WFD is compensated. Furthermore, the residual WFD compensated by the global calibration method and the multipoint calibration method comparing with the inherent WFD are shown in Figs. 9(e) and 9(f). Figure 9(g) illustrates the residual WFD after global calibration and multipoint calibration. The maximum phase value of the residual WFD compensated by the global calibration method is 0.364λ ($\lambda = 632.8$ nm), and the multipoint calibration method reduces it to 0.140λ.

The aperture of the LCoS device is not fully used in most applications. We usually need a circular aperture or a square aperture. The PV values of the residual WFD in different aperture sizes in Figs. 9(e) and 9(f) are calculated as shown in Fig. 10. Different aperture sizes are defined as shown in Fig. 4(a). It is shown in Fig. 10 that the PV values in full aperture, square aperture, and circular aperture by global

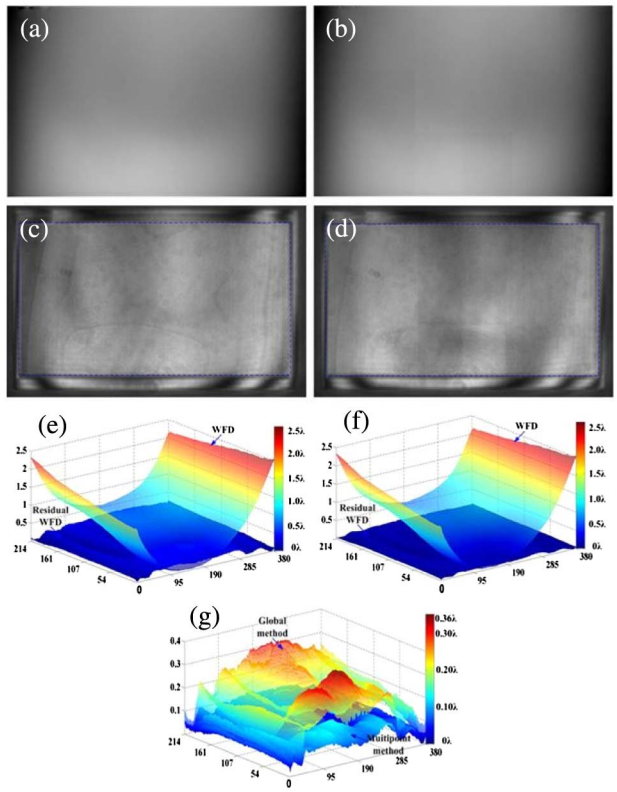

Fig. 9. 2D gray patterns calculated by Eq. (4) using (a) the global phase retardance function and (b) the multipoint phase retardance function to compensate the inherent WFD caused by the LCoS device. (c), (d) Interferograms after compensation of inherent WFD corresponding to the 2D gray patterns in (a) and (b). (e), (f) Comparison the inherent WFD with the residual WFD compensated by the global calibration method and the multipoint calibration method, respectively. (g) Comparison with the residual WFD compensated by the global calibration method and the multipoint calibration method.

phase retardance calibration are 0.364λ, 0.260λ, and 0.258λ ($\lambda = 632.8$ nm), respectively. The multipoint calibration method reduces the PV values in full aperture, square aperture, and circular aperture further to 0.140λ, 0.126λ, and 0.125λ.

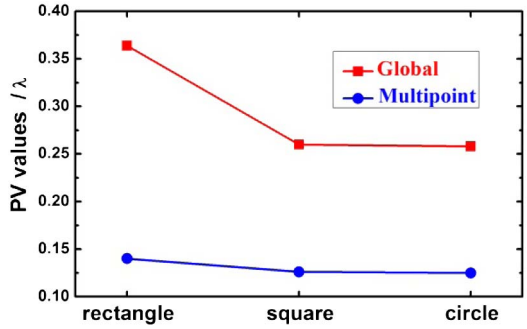

Fig. 10. PV values of the residual WFD in different aperture sizes after phase compensation using the global calibration method and the multipoint calibration method.

6. GENERATION OF 2D AIRY BEAMS

A. 2D Airy Beams

To show the improved optical performance of the LCoS device after compensation of SPNU, the device is utilized to produce a 2D Airy beam in Fourier space. The finite-energy 2D Airy packets at the origin ($z = 0$) can be expressed as

$$\phi(x, y, z = 0) = \mathrm{Ai}\left(\frac{x}{x_0}\right)\mathrm{Ai}\left(\frac{y}{y_0}\right)\exp\left(\frac{x}{w_1}\right)\exp\left(\frac{y}{w_2}\right). \quad (5)$$

The Fourier transformation of the finite-energy 2D Airy packets is Gaussian and involves a cubic phase, which can be expressed as

$$\Phi(k_x, k_y) \propto \exp[a(k_x^2 + k_y^2)]\exp\left[\frac{i(k_x^3 + k_y^3)}{3}\right]. \quad (6)$$

According to Eq. (6), a finite-energy 2D Airy beam can be generated from a Gaussian beam imposing a cubic phase through a Fourier transformation.

B. Experiment Results

Figure 11 shows the schematic of the diffraction optical system used to generate 2D Airy beams. First, a collimated He–Ne (632.8 nm) laser goes through a spatial filtering system, which comprises lens 1, 2, and a pinhole. Then, the beam passes through a beam splitter and a polarizer and gets to the LCoS device. In phase-only modulation mode, the incident beam is modulated by the LCoS device, which is loaded a gray mask of 2D Airy beam calculating from Eq. (6) as shown in Fig. 11. After that, the beam is Fourier-transformed by Fourier lens 3, whose focal length f is 700 mm. Finally, a 2D Airy beam can be observed by a CCD placed at the focus of lens 3. In order to separate the zero-order diffraction, we superimpose a blazed grating, with a phase range of -20π to 20π, onto the cubic phase mask of a single 2D Airy beam [17].

The generated 2D Airy beams without compensation of SPNU and with compensation of SPNU are shown in Figs. 12(a) and 12(b). Detailed views of the corresponding 2D Airy beams are shown as an inset in Figs. 12(a) and 12(b).

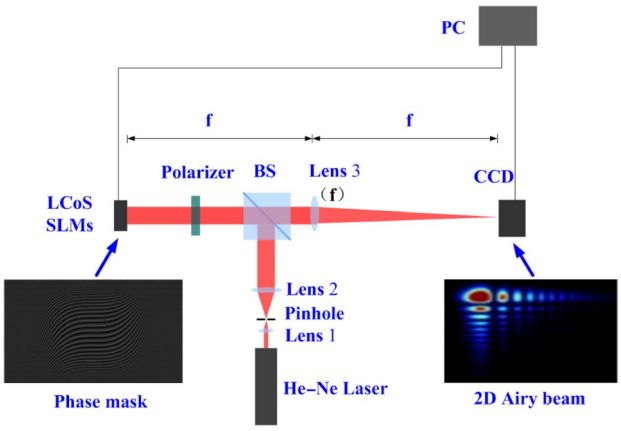

Fig. 11. Schematic of the optical system to generate 2D Airy beams on the LCoS device, where the He–Ne laser is a collimated 632.8 nm laser, BS is the beam splitter, lens 1, the pinhole, and lens 2 are a spatial filter, the focal length of lens 3 is 700 mm, and the distance between the LCoS device and lens 3 is also 700 mm.

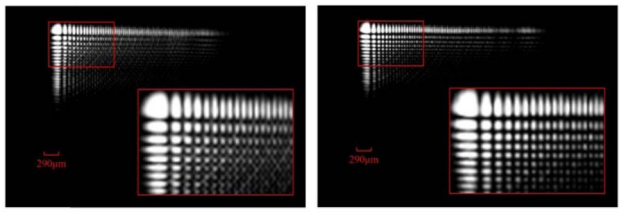

Fig. 12. Results of the generated 2D Airy beams in Fourier space by loading the cube phase patterns on the LCoS device (a) before compensation of SPNU and (b) after compensation of SPNU. The red rectangles in (a) and (b) denote the detailed views of the corresponding 2D Airy beams shown as an inset.

Figures 12(a) and 12(b) demonstrate that the qualities of the generated 2D Airy beams are improved when the SPNU of the LCoS device is compensated. It is noted that more energies reside in the centers of the intensity lobes, and the profiles of energies are more clear and regular as shown in Fig. 12(b) than that shown in Fig. 12(a).

7. CONCLUSIONS

An efficient multipoint calibration method to improve the optical performance of the LCoS device by fully compensating the SPNU using a Fizeau interferometer is presented. Compensation results show that this method can efficiently correct the SPNU of the device. The residual WFD across the aperture after phase compensation by the multipoint calibration method drops to 0.140λ from 2.5λ at the wavelength of 632.8 nm. In generation experiments of the 2D Airy beams, it is shown that the qualities of the generated 2D Airy beams are improved when the SPNU is compensated. The calibration method that we proposed is quite simple and time-saving, which can be successfully applied in the initial phase retardance calibration of the LCoS device. Moreover, it compensates the WFD caused by the thickness variations of the LC layer and glass substrate and the curvature of the silicon backplane. It is worth mentioning that a grid of 3×6 cells is defined onto the aperture by the multipoint calibration example in this paper. By increasing the number of cells, a further improvement in the optical performance of the device would be achieved.

FUNDING. National High Technology Research and Development Program of China (2015AA042402).

REFERENCES

1. W. Harm, C. Roider, S. Bernet, and M. Ritsch-Marte, "Tilt-effect of holograms and images displayed on a spatial light modulator," Opt. Express **23**, 30497–30511 (2015).
2. Z. Zhang, Z. You, and D. Chu, "Fundamentals of phase-only liquid crystal on silicon (LCOS) devices," Light Sci. Appl. **3**, e213 (2014).
3. H. Huang, T. Inoue, and H. Tanaka, "Stabilized high-accuracy correction of ocular aberrations with liquid crystal on silicon spatial light modulator in adaptive optics retinal imaging system," Opt. Express **19**, 15026–15040 (2011).
4. M. J. Booth, "Adaptive optical microscopy: the ongoing quest for a perfect image," Light Sci. Appl. **3**, e165 (2014).

5. J. Albero, P. García-Martínez, J. L. Martínez, and I. Moreno, "Second order diffractive optical elements in a spatial light modulator with large phase dynamic range," Opt. Lasers Eng. **51**, 111–115 (2013).
6. T. Čižmár, M. Mazilu, and K. Dholakia, "*In situ* wavefront correction and its application to micromanipulation," Nat. Photonics **4**, 388–394 (2010).
7. A. Hermerschmidt, S. Krüger, T. Haist, S. Zwick, M. Warber, and W. Osten, "Holographic optical tweezers with real-time hologram calculation using a phase-only modulating LCOS-based SLM at 1064 nm," Proc. SPIE **6905**, 690508 (2008).
8. T. Kozacki, "Holographic display with tilted spatial light modulator," Appl. Opt. **50**, 3579–3588 (2011).
9. D. Engström, M. Persson, J. Bengtsson, and M. Goksör, "Calibration of spatial light modulators suffering from spatially varying phase response," Opt. Express **21**, 16086–16103 (2013).
10. Holoeye Photonics AG and Holoeye Corporation, "PLUTO-VIS-020 phase-only SLM: (530–640nm)," http://www.holoeye.com/wp-content/uploads/PLUTO-VIS-020.pdf.
11. D. K. Yang and S. T. Wu, *Fundamentals of Liquid Crystal Devices* (Wiley, 2006), Chap. 2.
12. X. Xun and R. W. Cohn, "Phase calibration of spatially nonuniform spatial light modulators," Appl. Opt. **43**, 6400–6406 (2004).
13. Z. Zhang, H. Yang, B. Robertson, M. Redmond, M. Pivnenko, N. Collings, W. A. Crossland, and D. Chu, "Diffraction based phase compensation method for phase-only liquid crystal on silicon devices in operation," Appl. Opt. **51**, 3837–3846 (2012).
14. J. L. Harriman, A. Linnenberger, and S. A. Serati, "Improving spatial light modulator performance through phase compensation," Proc. SPIE **5553**, 58–67 (2004).
15. L. Teng, M. Pivnenko, B. Robertson, R. Zhang, and D. Chu, "A compensation method for the full phase retardance nonuniformity in phase-only liquid crystal on silicon spatial light modulators," Opt. Express **22**, 26392–26402 (2014).
16. J. Otón, P. Ambs, M. S. Millán, and E. Pérez-Cabré, "Multipoint phase calibration for improved compensation of inherent wavefront distortion in parallel aligned liquid crystal on silicon displays," Appl. Opt. **46**, 5667–5679 (2007).
17. X. Wang, Q. Li, and Q. Wang, "Arbitrary scanning of the Airy beams using additional phase grating with cubic phase mask," Appl. Opt. **51**, 6726–6731 (2012).

159.226.165.13 {ts '2017-06-22 23:02:25'}